EUROPEAN ORGANIZATION FOR NUCLEAR RESEARCH

**Proposal to the ISOLDE and Neutron Time-of-Flight Committee**

# Coulomb excitation of neutron-deficient $^{78,80}$Sr and deformation around N=Z=40

September 27, 2022

J. Henderson[1], R. Wadsworth[2], J. N. Orce[3], W. N. Catford[1], D. T. Doherty[1], J. Heery[1], G. Lotay[1], Z. Podolyak[1], P. Regan[1], R. Russell[1], C. J .Barton[2], M. A. Bentley[2], D. G. Jenkins[2], L. P. Gaffney[4], S. Kisyov[5], C. Y. Wu[5], J. M. Allmond[6], T. Gray[6], K. Hadynska-Klek[7], M. Komorowska[7], P. J. Napiorkowski[7], K. Wrzosek-Lipska[7], C. Andreoiu[8], P. Spagnoletti[8], F. Wu[8], J. Smallcombe[9], P. Ruotsalainen[10], P. Garrett[11], M. Zielinska[12], G. Hackman[13], F. Browne[14], T. Kröll[15], N. Warr[16]

[1] *University of Surrey, Guildford, UK;* [2] *University of York, York, UK;* [3] *University of the Western Cape, South Africa;* [4] *University of Liverpool, Liverpool, UK;* [5] *Lawrence Livermore National Laboratory, USA;* [6] *Oak Ridge National Laboratory, USA;* [7] *Heavy Ion Laboratory, University of Warsaw, Poland;* [8] *Simon Fraser University, Canada;* [9] *JAEA, Japan;* [10] *University of Jyvaskyla, Finland;* [11] *University of Guelph, Canada;* [12] *CEA Saclay, France;* [13] *TRIUMF, Canada;* [14] *CERN;* [15] *TU Darmstadt, Germany;* [16] *Universität zu Köln, Germany*

**Spokespersons:** J. Henderson (jack.henderson@surrey.ac.uk); R. Wadsworth (bob.wadsworth@york.ac.uk); J. N. Orce (jnorce@uwc.ac.za)
**Contact person:** Frank Browne (frank.browne@cern.ch)

**Abstract:** We propose to study the strong region of deformation around $N = Z = 40$ by performing a Coulomb-excitation measurement on neutron-deficient $^{78,80}$Sr. Understanding $E2$ matrix elements in these isotopes, lying just South of $^{80}$Zr, is essential to the elucidation of the emergence this island of deformation.

**Requested shifts:** 24 shifts
**Installation:** MINIBALL + CD-only

# 1 Physics case

Quadrupole deformation is ubiquitous in atomic nuclei but the extent to which it contributes to the structure of individual nuclei varies dramatically across the nuclear landscape. Regions in the vicinity of closed shells exhibit only weak deformation in their low-lying states, while in the mid-shell it emerges as a dominant driver in the low-lying level structure, often with competing shape minima giving rise to coexisting configurations [1]. This evolution from near-sphericity towards strongly-deformed structure provides a rich and exceptionally challenging laboratory for our understanding of nuclei.

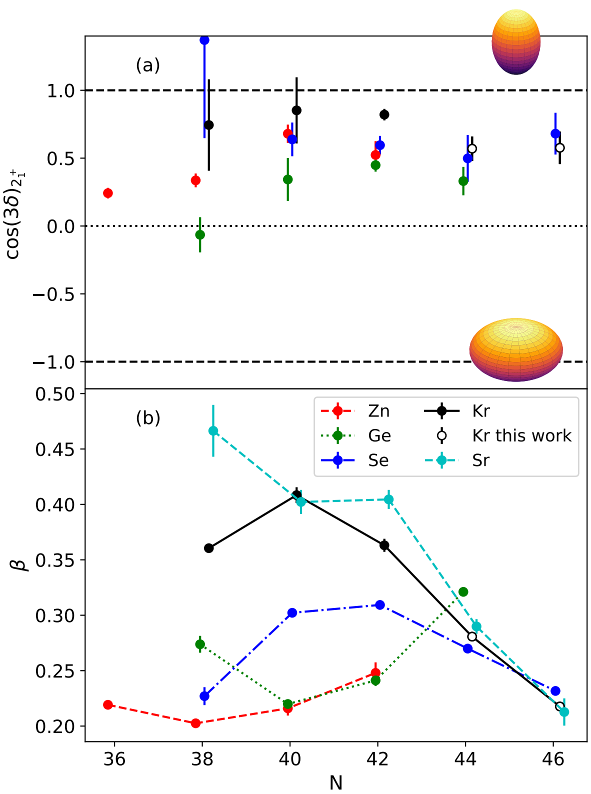


Figure 1: (a) $\cos(3\delta)$ of neutron-deficient Zn, Ge, Sr and Kr isotopes where $\delta \approx \gamma$. See text for definition. An evolution towards $\gamma = 1$, corresponding to maximally prolate deformation is seen. (b) $\beta$ the same isotopic chains but now incorporating Sr isotopes. The increase in deformation into the Kr and Sr isotopes is clear. Figure taken from Ref. [2].

In low- and mid-mass nuclei there are relatively few concentrated regions of strong deformation, often localised around e.g. $\alpha$ clustering and breakdowns of single-particle structure. Perhaps the lightest conventional region of strong ground-state deformation is that around N=Z=40, where the large valence space allows for its emergence. While the magnitude of the nuclear deformation has been experimentally established in fast beam experiments (e.g. Refs. [3, 4]), its form (e.g. prolate vs oblate vs triaxial) remains unknown. This mystery is exacerbated by the complex single-particle structure in the region, with many contributing configurations giving rise to a prediction of multi-fold shape-coexistence consisting of a variety of forms of deformation [5]. Indeed, within a spherical basis, forty constitutes a semi-magic number, as highlighted by the quasi-doubly-magic nature of $^{90}$Zr (e.g. Ref. [6]).

The evolution of deformation towards $N = Z = 40$ can be seen in experimental systematics. Making use of a simplified relation [7] from the Kumar-Cline [8, 9] sum rules one can approximate for even-even nuclei

$$\cos(3\delta) \approx -\frac{Q_s(2_1^+)}{\frac{2}{7}\sqrt{\frac{16\pi}{5} \times B(E2; 0_1^+ \to 2_1^+)}}. \tag{1}$$

Here, $\delta$ is a charge analogue of the Bohr $\gamma$ parameter. The two can be equated under the assumption of identical charge and matter distributions. Here, $Q_s(2_1^+)$ is the spectroscopic quadrupole moment of the first $2^+$ state.

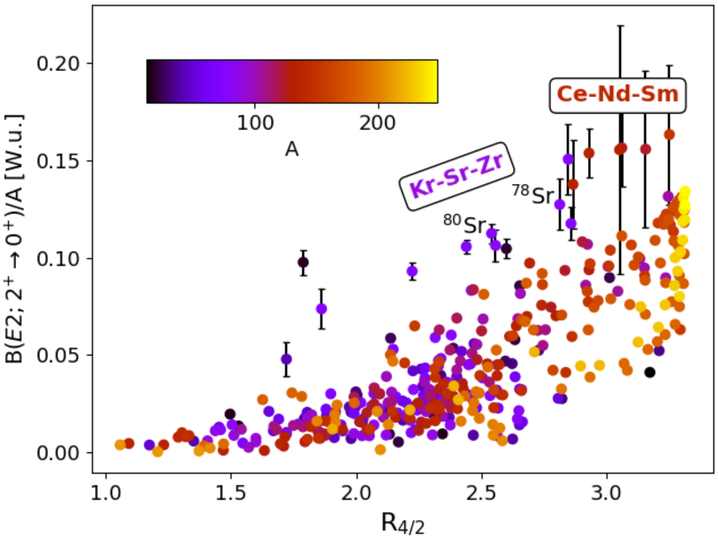


Figure 2: $B(E2; 2^+ \to 0^+)$ values divided by nucleon number, plotted against the ratio of $4^+$ and $2^+$ energies across the nuclear landscape. An evolution from spherical nuclei (low B(E2), $R_{4/2} \sim 1$) to axial rotors (large B(E2), $R_{4/2} \sim 3.3$) is visible, as well as two highlighted outlying regions. The nuclei of interest for the present proposal are indicated. Data taken from Ref. [10].

The data are shown in Fig. 1, with $\cos(3\delta)$ plotted for Zn, Ge, Se and Kr isotopes in (a) and alongside $\beta$ (b) including Sr isotopes as well. The evolution shown in the data is clear: as one moves towards $N = Z = 40$ the nuclear deformation becomes stronger (larger $\beta$) and moves towards a maximally prolate solution ($\cos(3\delta) = 1$). If this evolution persists, one would expect Sr and Zr isotopes to be strongly deformed and axially prolate.

As previously mentioned, the role of shape coexistence and mixing also remains paramount in this region. Within level systematics and transition strengths there exist some peculiarities that may point to such behaviours. Figure 2 shows $B(E2; 2^+ \to 0^+)$ values in Weisskopf units divided by nucleon number, plotted against the $R_{4/2}$ ratio for nuclei across the nuclear landscape. Outside a general evolution of behaviour towards a constant $B(E2; 2^+ \to 0^+)/A$ at $R_{4/2} \sim 3.3$, there are two outlying regions: neutron-deficient Kr-Sr-Zr isotopes and neutron-deficient Ce-Nd-Sm. Perhaps the most obvious explanation for this deviation is the presence of significant shape mixing, however to date there is no evidence of low-lying coexisting configurations in neutron-deficient Sr and Zr (such states have been identified in Kr, however [11]). This explanation would appear to be in conflict with, or at least significantly complicate, the aforementioned picture of evolution towards a stable axial deformation.

On the other hand, recent theoretical work [12] made use of state-of-the-art many body methods to investigate the region, demonstrating the crucial role of quasi-SU(3) partners ($g_{9/2}$-$d_{5/2}$) in driving collectivity in the mass region. Indeed, this is found to be enhanced thanks to a three-fold enhancement in nn, np and pp couplings, thanks to the proximity of the line of $N = Z$. Thanks to the inclusion of these quasi-SU(3) partners, the B(E2) enhancement in Fig. 2 is reproduced [13], although the simultaneous reduction in $R_{4/2}$ is not. It is possible, therefore, that the dramatic evolution towards axial prolate deformation in Fig. 1 and the apparently systematic deviation in Fig. 2 represent two features arising from the same, heavily-enhanced, quadrupole deformation.

In resolving the enigma of nuclear shapes in neutron-deficient $N \sim Z \sim 40$ nuclei, $E2$ matrix elements are the acid test. In particular, as shown in Eq. 1, diagonal matrix elements (spectroscopic quadrupole moments) and transition matrix elements ($B(E2)$ values) can be compared in order to disentangle the intrinsic deformation of the nucleus in question. To extract these values, we propose performing a safe Coulomb-excitation measurement of $^{78,80}$Sr. In doing so, we will also have strong sensitivity to low-lying, off-yrast $2^+$ states, and potential sensitivity to off-yrast $0^+$ states, which are themselves symptomatic of (tri)axiality and shape-coexistence, respectively.

# 2 Experiments

The isotopes of interest for the present proposal are $^{78,80}$Sr, which have been previously produced at ISOLDE. These isotopes are challenging to investigate due to the anticipated presence of significant rubidium contamination. Two potential techniques for suppressing this contamination have been considered:

- **LIST:** The Laser Ion Source and Trap provides a mechanism for suppressing surface-ionised contaminants through the use of a positively biased repeller electrode placed immediately at the exit of the hot cavity. Atoms that are primarily ionised within the target, such as Rb, are therefore suppressed. Neutral atoms proceed unperturbed into the LIST volume, where they are selectively laser ionised. Due to the relatively strong surface-ionisation of Sr, this method is expected to result in a significant loss in atoms of interest, by a factor of about 50. Nonetheless, the Rb suppression is anticipated to be about a factor of 1000, making the proposed experiment viable through comparison between "laser-on" and "laser-off" data sets.

- **Molecular extraction:** The extraction of Sr as a fluoride has previously been demonstrated and was found to be very efficient, even without F-injection. These molecules will then be broken up in the EBIS and reaccelerated, suppressing the Rb contamination completely. The use of SrF would, however, also result in the extraction of other isobaric fluoride molecules that might provide an alternative form of contamination.

For the purpose of this proposal, we assume the a beam extracted with LIST, with a LIST extraction efficiency of 2%, a charge breeding efficiency of 5%, an average integrated proton current of 1.5 $\mu$A and a suppression factor for Rb of 1000. SC yields from the ISOLDE yield database were used. The beams, with rubidium contamination suppressed, will be accelerated to the safe Coulomb-excitation limit of 4.26 MeV/u and impinged upon $^{196}$Pt and $^{198}$Pt foils, for $^{78}$Sr and $^{80}$Sr, respectively, and $^{208}$Pb for both nuclei, located at the target position of the Miniball HPGe array. The different Pt isotopes were selected to ensure $\gamma$-decays from target excitations did not interfere with $\gamma$-rays from the nuclei of interest, while allowing for normalization to the target excitation. The $^{208}$Pb

| | | | | | | | |
|---|---|---|---|---|---|---|---|
| | Counts / $5 \times 10^5$ pps / day | | | | | | |
| $^{80}$Sr | $2_1^+$ | $4_1^+$ | $0_1^+$ | $2_2^+$ | $2_3^+$ | $6_1^+$ | $8_1^+$ |
| | $2.2 \times 10^5$ | $3.4 \times 10^4$ | 230 | 340 | 55 | 7900 | 730 |
| | Counts / $3 \times 10^3$ pps / day | | | | | | |
| $^{78}$Sr | $2_1^+$ | $4_1^+$ | $2_2^+$* | | | | |
| | $1.8 \times 10^3$ | 260 | 4 | | | | |

Table 1: Estimated yields for the proposed measurement for $^{80}$Sr and $^{78}$Sr. Yields per day are presented in terms of average intensities ($1 \times 10^5$ pps and $1 \times 10^4$ pps assumed for $^{80,78}$Sr, respectively). Where literature transition matrix elements were not available, $\langle i|\, E2\,|f\rangle = 0.1$ eb was assumed. An example $2_2^+$ state in $^{78}$Sr was included at 1 MeV excitation energy. Calculations were performed using the GOSIA [14] code based on evaluated data [10], where available. All diagonal matrix elements were set to zero. Miniball photopeak efficiencies [15] have been accounted for.

target provides an exceptionally clean spectrum and can be analysed simultaneously to the Pt data, ensuring no loss in sensitivity. Scattered beam- and target-like particles will be detected downstream in an annular silicon detector, providing wide coverage in the centre-of-mass frame. We assume intensities for $^{78}$Sr ($^{78}$Rb) and $^{80}$Sr ($^{80}$Rb) of $3\times10^3$ pps ($1.8 \times 10^4$ pps) and $5 \times 10^5$ pps ($1.4 \times 10^6$ pps), respectively.

Clearly, Rb contamination remains significant, even with LIST suppression, but can managed empirically. Firstly, the experiment will be run in alternating configurations: in the first ("signal" mode) the lasers will be unblocked, in the second ("background" mode) the lasers will be blocked. The signal mode will contain enhanced Sr, alongside surface-ionised Sr and Rb. The background mode will contain only the surface-ionised Sr and Rb. Through appropriate (empirical) subtractions, a "pure" Rb spectrum can therefore be constructed and subtracted from the data to yield clean Sr spectra. This capability can be automated to alternate between laser on/off every super-cycle, ensuring that the signal and background data are taken under the most similar conditions practicable. Secondly, while the Rb yields remain significant, as odd-odd nuclei, the excitation is anticipated to be considerably more fractured than for the Sr. Contributions from the Rb contamination that actively interfere with the Sr analysis are therefore expected to be minimal. Finally, through online monitoring of the composition in an ionisation chamber, the target normalization can be corrected for the presence of the Rb contamination. Based on the above assumptions, anticipated daily yields are summarised in Table 1 for the two Sr isotopes.

In the calculations presented in Table 1, a hypothetical (indicated by *) second $2^+$ state was included at 1 MeV excitation energy, connected to both the ground- and first-excited-state by a 0.1 eb $E2$ matrix element. With the goal of observing a state such as this, we request two days of $^{78}$Sr impinged upon a $^{208}$Pb target, for maximum cleanliness in the $\gamma$-ray spectrum, allowing for the observation of the $\sim$ 10 counts predicted. We additionally request a single day of $^{78}$Sr to be impinged upon a $^{196}$Pt target, allowing for absolute $E2$ matrix elements to be determined for a total of three days of $^{78}$Sr running in "signal" mode. We request a single day of $^{80}$Sr, during which both $^{208}$Pb and $^{198}$Pt targets will be used. Finally, we match the above time with an equivalent period (three days of $^{78}$Sr and one of $^{80}$Sr) of laser-off time, in order to perform a statistically precise subtraction of the surface-ionised contamination.

This request will allow for:

- the determination of $Q(2^+)$ values in both nuclei,
- $Q(J^\pi)$ values for higher lying states in $^{80}$Sr,
- independent confirmation of $B(E2)$ values previously determined from lifetime measurements,
- a search for higher-lying excited $2^+$ and $0^+$ states in both nuclei.

The above combined information, viewed together, will serve to quantify the roles of deformation, such as triaxiality and shape coexistence, in the neutron-deficient $N \sim Z \sim 40$ region of the nuclear landscape.

**Summary of requested shifts: In total we request six days (eighteen shifts) of $^{78}$Sr and two days (six shifts) of $^{80}$Sr.**

# References


[1] Kris Heyde and John L. Wood. *Rev. Mod. Phys.*, 83:1467–1521, Nov 2011.

[2] S. A. Gillespie, J. Henderson, K. Abrahams, F. A. Ali, L. Atar, G. C. Ball, N. Bernier, S. S. Bhattcharjee, R. Caballero-Folch, M. Bowry, A. Chester, R. Coleman, T. Drake, E. Dunling, A. B. Garnsworthy, B. Greaves, G. F. Grinyer, G. Hackman, E. Kasanda, R. LaFleur, S. Masango, D. Muecher, C. Ngwetsheni, S. S. Ntshangase, B. Olaizola, J. N. Orce, T. Rockman, Y. Saito, L. Sexton, P. Šiurytė, J. Smallcombe, J. K. Smith, C. E. Svensson, E. Timakova, R. Wadsworth, J. Williams, M. S. C. Winokan, C. Y. Wu, and T. Zidar. *Phys. Rev. C*, 104:044313, Oct 2021.

[3] R. D. O. Llewellyn, M. A. Bentley, R. Wadsworth, H. Iwasaki, J. Dobaczewski, G. de Angelis, J. Ash, D. Bazin, P. C. Bender, B. Cederwall, B. P. Crider, M. Doncel, R. Elder, B. Elman, A. Gade, M. Grinder, T. Haylett, D. G. Jenkins, I. Y. Lee, B. Longfellow, E. Lunderberg, T. Mijatović, S. A. Milne, D. Muir, A. Pastore, D. Rhodes, and D. Weisshaar. *Phys. Rev. Lett.*, 124:152501, 2020.

[4] A. Lemasson, H. Iwasaki, C. Morse, D. Bazin, T. Baugher, J. S. Berryman, A. Dewald, C. Fransen, A. Gade, S. McDaniel, A. Nichols, A. Ratkiewicz, S. Stroberg, P. Voss, R. Wadsworth, D. Weisshaar, K. Wimmer, and R. Winkler. *Phys. Rev. C*, 85:041303, 2012.

[5] Tomás R. Rodríguez and J. Luis Egido. *Physics Letters B*, 705(3):255–259, 2011.

[6] P. E. Garrett, W. Younes, J. A. Becker, L. A. Bernstein, E. M. Baum, D. P. DiPrete, R. A. Gatenby, E. L. Johnson, C. A. McGrath, S. W. Yates, M. Devlin, N. Fotiades, R. O. Nelson, and B. A. Brown. *Phys. Rev. C*, 68:024312, Aug 2003.

[7] J. Henderson. *Phys. Rev. C*, 102:054306, Nov 2020.

[8] K. Kumar. *Physical Review Letters*, 28:249, 1972.

[9] D. Cline. *Annual Review of Nuclear and Particle Science*, 36:681, 1986.

[10] NNDC. Evaluated Nuclear Structure Data File (ENSDF).

[11] E. Clément, A. Görgen, W. Korten, E. Bouchez, A. Chatillon, J.-P. Delaroche, M. Girod, H. Goutte, A. Hürstel, Y. Le Coz, A. Obertelli, S. Péru, Ch. Theisen, J. N. Wilson, M. Zielińska, C. Andreoiu, F. Becker, P. A. Butler, J. M. Casandjian, W. N. Catford, T. Czosnyka, G. de France, J. Gerl, R.-D. Herzberg, J. Iwanicki, D. G. Jenkins, G. D. Jones, P. J. Napiorkowski, G. Sletten, and C. N. Timis. *Phys. Rev. C*, 75:054313, 2007.

[12] K. Kaneko, N. Shimizu, T. Mizusaki, and Y. Sun. *Phys. Lett. B*, 817:136286, 2021.

[13] K. Kaneko. Private Communication.

[14] T. Czosnyka, D. Cline, and C. Y. Wu. *Bull. Am. Phys. Soc.*, 28:745, 1983.

[15] N. Warr et al. *Eur. Phys. J. A*, 49:40, 2013.

# Appendix

**DESCRIPTION OF THE PROPOSED EXPERIMENT**

The experimental setup comprises: (*name the fixed-ISOLDE installations, as well as flexible elements of the experiment*)

| Part of the | Availability | Design and manufacturing |
|---|---|---|
| MINIBALL + only CD | ☒ Existing | ☒ To be used without any modification |
| [$^{78}$Sr experiment/ equipment] | ☒ Existing | ☐ To be used without any modification<br>☐ To be modified |
| | ☐ New | ☐ Standard equipment supplied by a manufacturer<br>☐ CERN/collaboration responsible for the design and/or manufacturing |
| [$^{80}$Sr experiment/ equipment] | ☒ Existing | ☐ To be used without any modification<br>☐ To be modified |
| | ☐ New | ☐ Standard equipment supplied by a manufacturer<br>☐ CERN/collaboration responsible for the design and/or manufacturing |
| [insert lines if needed] | | |

HAZARDS GENERATED BY THE EXPERIMENT Hazards named in the document relevant for the fixed MINIBALL + only CD installation.

Additional hazards:

| Hazards | [Part 1 of experiment/ equipment] | [Part 2 of experiment/ equipment] | [Part 3 of experiment/ equipment] |
|---|---|---|---|
| **Thermodynamic and fluidic** | | | |
| Pressure | [pressure][Bar], [volume][l] | | |
| Vacuum | | | |
| Temperature | [temperature] [K] | | |
| Heat transfer | | | |
| Thermal properties of materials | | | |
| Cryogenic fluid | [fluid], [pressure][Bar], [volume][l] | | |
| **Electrical and electromagnetic** | | | |
| Electricity | [voltage] [V], [current][A] | | |
| Static electricity | | | |
| Magnetic field | [magnetic field] [T] | | |
| Batteries | ☐ | | |

| | | | |
|---|---|---|---|
| Capacitors | ☐ | | |
| **Ionizing radiation** | | | |
| Target material [material] | | | |
| Beam particle type (e, p, ions, etc) | $^{78}$Sr + $^{78}$Rb | $^{80}$Sr + $^{80}$Rb | |
| Beam intensity | $1 \times 10^6$ | $1 \times 10^7$ | |
| Beam energy | 4.26 MeV/u | 4.26 MeV/u | |
| Cooling liquids | [liquid] | | |
| Gases | [gas] | | |
| Calibration sources: | ☐ | | |
| • Open source | ☐ | | |
| • Sealed source | ☒ [ISO standard] | | |
| • Isotope | $^{60}$Co, $^{152}$Eu | | |
| • Activity | | | |
| Use of activated material: | | | |
| • Description | ☐ | | |
| • Dose rate on contact and in 10 cm distance | [dose][mSV] | | |
| • Isotope | | | |
| • Activity | | | |
| **Non-ionizing radiation** | | | |
| Laser | | | |
| UV light | | | |
| Microwaves (300MHz-30 GHz) | | | |
| Radiofrequency (1-300 MHz) | | | |
| **Chemical** | | | |
| Toxic | [chemical agent], [quantity] | | |
| Harmful | [chem. agent], [quant.] | | |
| CMR (carcinogens, mutagens and substances toxic to reproduction) | [chem. agent], [quant.] | | |
| Corrosive | [chem. agent], [quant.] | | |
| Irritant | [chem. agent], [quant.] | | |
| Flammable | [chem. agent], [quant.] | | |
| Oxidizing | [chem. agent], [quant.] | | |
| Explosiveness | [chem. agent], [quant.] | | |
| Asphyxiant | [chem. agent], [quant.] | | |
| Dangerous for the environment | [chem. agent], [quant.] | | |
| **Mechanical** | | | |

| | | | |
|---|---|---|---|
| Physical impact or mechanical energy (moving parts) | [location] | | |
| Mechanical properties (Sharp, rough, slippery) | [location] | | |
| Vibration | [location] | | |
| Vehicles and Means of Transport | [location] | | |
| **Noise** | | | |
| Frequency | [frequency],[Hz] | | |
| Intensity | | | |
| **Physical** | | | |
| Confined spaces | [location] | | |
| High workplaces | [location] | | |
| Access to high workplaces | [location] | | |
| Obstructions in passageways | [location] | | |
| Manual handling | [location] | | |
| Poor ergonomics | [location] | | |

Hazard identification:

Average electrical power requirements (excluding fixed ISOLDE-installation mentioned above): [make a rough estimate of the total power consumption of the additional equipment used in the experiment]: ... kW